Juice/SWI during the Lunar-Earth-Gravity-Assist (LEGA). I. General overview

Paul Hartogh[1], Ladislav Rezac[1], Thibault Cavalié[2], Christopher Jarchow[1], Raphael Moreno[3], Ali Schulz-Ravanbakhsh[1], Alberto Carrasco Gallardo[1], Borys Dabrowski[1], Samuel Goodyear[1], Miriam Rengel[1], , Fabrice Herpin[2], Yasuko Kasai[4], Mikko Kotiranta[5], Emmanuel Lellouch[3], Axel Murk[5], Michael Olberg[7], Slawomira Szutowicz[6], Eva Wirström[7].

[1]Max-Planck-Institut für Sonnensystemforschung, 37077 Göttingen, Germany
[2]Univ. Bordeaux, CNRS, LAB, UMR 5804, F-33600 Pessac, France
[3]LIRA – Laboratoire d'Instrumentation et de Recherche en Astrophysique, Observatoire de Paris, Section de Meudon, 5, place Jules Janssen – 92195 MEUDON, France
[4]National Institute of Information and Communications Technology, 4-2-1 Nukuikita-Machi, Koganei, Tokyo, 184-8795, Japan
[5]Institute of Applied Physics, University of Bern, Sidlerstrasse 5, Bern, 3012, Bern, Switzerland
[6]Centrum Badań Kosmicznych PAN, Bartycka 18A, Warsaw, Poland
[7]Department of Space, Earth, and Environment, Chalmers University of Technology, 412 96 Gothenburg, Sweden

Correspondence to: Paul Hartogh (hartogh@mps.mpg.de)

Abstract. The Jupiter Icy moons Explorer (Juice) was the first spacecraft ever that performed a combined gravity assist using both the Moon and Earth in succession. The double flyby required highly precise navigation to succeed. The LEGA allowed Juice to make a shortcut through the inner solar system on its way to Jupiter, using less fuel than would have been otherwise required. On August 19, 2024, Juice had its closest approach to the Moon. This first part of the manoeuvre accelerated the spacecraft by approximately 0.9 km/s relative to the Sun. On August 20, 2024, the spacecraft swung past Earth. This second part of the manoeuvre reduced the spacecraft's speed by 4.8 km/s relative to the Sun. This was a unique opportunity for its payloads to observe the Moon and Earth from a close distance as both calibration and science targets. The Submillimetre Wave Instrument (SWI), a dual channel heterodyne spectrometer observed both targets in two far-infrared bands around 500 and 250 µm wavelength in order to characterize and calibrate the overall performance of the instrument, including its receiver frontend, spectrometer backend and telescope mechanisms. In addition, the commanding pipeline and operations processes of the instrument were also tested close to its full range of flexibility using the relevant pipelines. In this paper we provide a contextual description of physical and functional characteristics of SWI, its operational principles and in-flight calibration activities during LEGA.

1 Introduction

The European Space Agency's (ESA) JUpiter ICy moons Explorer (Juice), launched on April 14, 2023, to study Jupiter and its icy moons, particularly Ganymede, Callisto, and Europa, will arrive after an 8.25-year cruise phase in the Jupiter system in 2031. After a tour in the Jupiter system with more than 30 satellite flybys (Boutonnet et al. 2024), Juice will become the first

spacecraft to orbit a moon of an outer planet when it enters orbit around Ganymede in 2034. Its goals are to investigate the evolution of potentially habitable worlds around gas giants, including studying the moons' subsurface oceans, and Jupiter's atmosphere and magnetosphere. The Juice science objectives and mission description details can be found in Grasset et al. (2013), Fletcher et al. (2023) and Tosi et al, (2024).

The cruise phase provides the opportunity for characterizing the performance, developing and testing the calibration, planning and the commanding pipelines of each instrument. Three months following the launch, the Near-Earth Commissioning Phase (NECP) took place. Regular Payload Checkout Windows (PCWs) are scheduled about every 6-months, to allow the instrument teams to perform routine instrument functional and health checks. Keys to the instrument performance verification are three planetary swing-bys. The Lunar-Earth Gravity Assist (LEGA) occurred in August 2024. It was a unique opportunity to calibrate the instrument and test scientific operations. Two additional Earth Gravity Assists (EGAs) will take place in September 2026 and January 2029.

The scientific payload of Juice consists of 10 instruments of which one is the Submillimetre Wave Instrument (SWI). It will sound the atmospheres of Jupiter and the Galilean moons in two Far Infrared bands covering the frequency ranges of 530 – 642 GHz and 1066 – 1275 GHz. Furthermore, it is designed to characterize the thermo-physical surface properties of Callisto, Ganymede and Europa during flybys and orbital phases (Ilyushin & Hartogh, 2020). A special feature of SWI is its very high spectral resolution of ~ 10^7. It allows to resolve all spectral lines details expected to be observable in the Jupiter system and retrieve from the precisely determined line shape information about the volume mixing ratio of the observed molecules along the line-of-sight (e.g. from pressure broadening), temperature and Doppler winds (e.g. Wirström et al.2020, Cavalié et al. 2021, 2023). SWI builds on the heritage of technologies developed over the last three decades including the Microwave Instrument for the Rosetta Orbiter (MIRO) (Beaudin et al, 1998 & Gulkis et al, 2007), the German Receiver for Astronomy at THz frequencies on the Stratospheric Observatory for Infrared Astronomy (SOFIA) (Güsten et al, 2000, Heymink et al, 2012) and the Heterodyne Instrument for the Far Infrared (HIFI) on the Herschel Space Observatory (de Graauw et al. 1998,2010). SWI was designed to fulfil the Juice mission science goals (see Hartogh et al 2026, in preparation).

2 Instrument description

SWI is a heterodyne spectrometer (Figure 1) that converts the THz frequency range into an intermediate frequency (IF) range around 6 GHz, by multiplying the signals received by the telescope (radio frequency, RF) with a frequency-tunable sinusoidal signal provided by the local oscillator (LO). The multiplying circuit is also called frequency mixer. The LO consists of frequency synthesizers that can be tuned in power to > 100 mW and in frequency between ~ 22 and 26.5 GHz in 1.875 MHz steps. The frequency synthesizers are integrated into the so-called Frequency Distribution Module (FDM) that is part of the

SWI Electronic Unit (EU). The FDM frequency synthesizers are locked to an 80 MHz low phase noise Ultra Stable Oscillator (USO).

Via radiation hard coaxial cables, the FDM output signals are fed to frequency triplers that are located on the warm part of the optical bench (Kotiranta et al, 2018) of the Telescope & Receiver Unit (TRU, Figure 2 left). The tripler output signals are amplified with E-band power amplifiers (PAs) in the 75 GHz range and frequency-doubled to 150 GHz**.** This "warm" LO part operates at temperatures between -50° C and 50° C and is interfaced with a thin-walled Titanium waveguides to the passively cooled part of the LO, consisting of another doubler (600 GHz receiver), and a quadrupler (1200 GHz, Treuttel et al. 2024), respectively. The 300 and 600 GHz LO signals are fed to the subharmonically-pumped (SHP) mixer LO-inputs. Starting from the FDM, the LO multiplication factors are 24 (600 GHz receiver) and 48 (1200 GHz receiver).

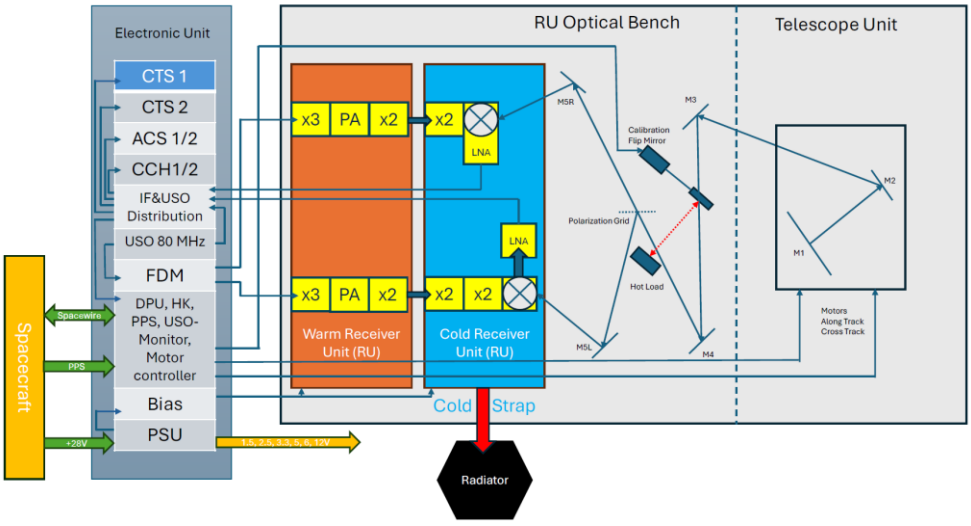

Figure 1: SWI block diagram (see text)

A single FDM frequency step converts to 45 (600 GHz receiver) and 90 (1200 GHz receiver) MHz in the SHP mixers. The IF-signals (mixer output) are amplified by low noise amplifiers (LNAs). While the 600 GHz receiver LNA is integrated into the mixer block, the 1200 GHz receiver LNA is connected to a separate LNA via a radiation hard coaxial cable. The cold frequency multipliers (doubler/quadrupler), mixers and LNAs are isolated from the optical bench via Titanium mechanical interfaces and

cooled via a pyrolytic graphite/copper cold strap with the SWI radiator. Operational temperatures of the cold part in space are between ~ 120 and 150 K, resulting in system temperatures of < 1500 and < 3000 K DSB (double sideband) for the 600/1200 GHz receivers.

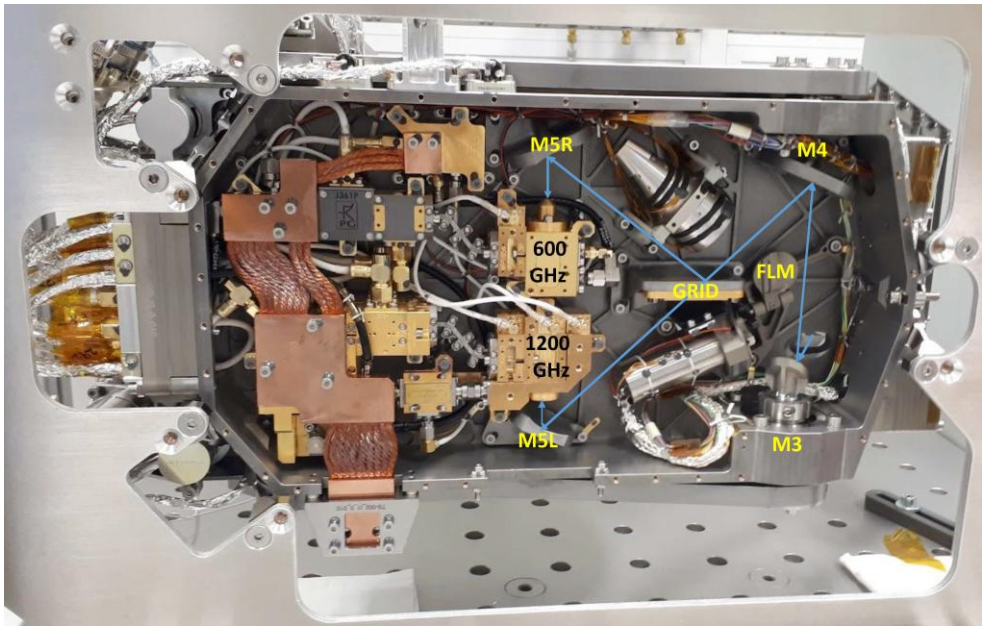

Figure 2: Receiver Unit (RU). The focused beam enters the RU through the elliptical hole in the lower right. The blue line indicates the beam path within the RU. It is first reflected by the M3 and M4 mirrors. A wire grid acts as a beam splitter so that the signals appear at the mirrors M5R (600 GHz receiver) and M5L (1200 GHz receiver), where they are focused into the mixer horns of the two receivers. A flip mirror (FLM) can be rotated into the beam so that the receivers "see" the hot calibration load (at ~ 240 K) rather than the signals from M1-M3. The cold calibration is done on the cosmic background (2.7 K) via the M1.

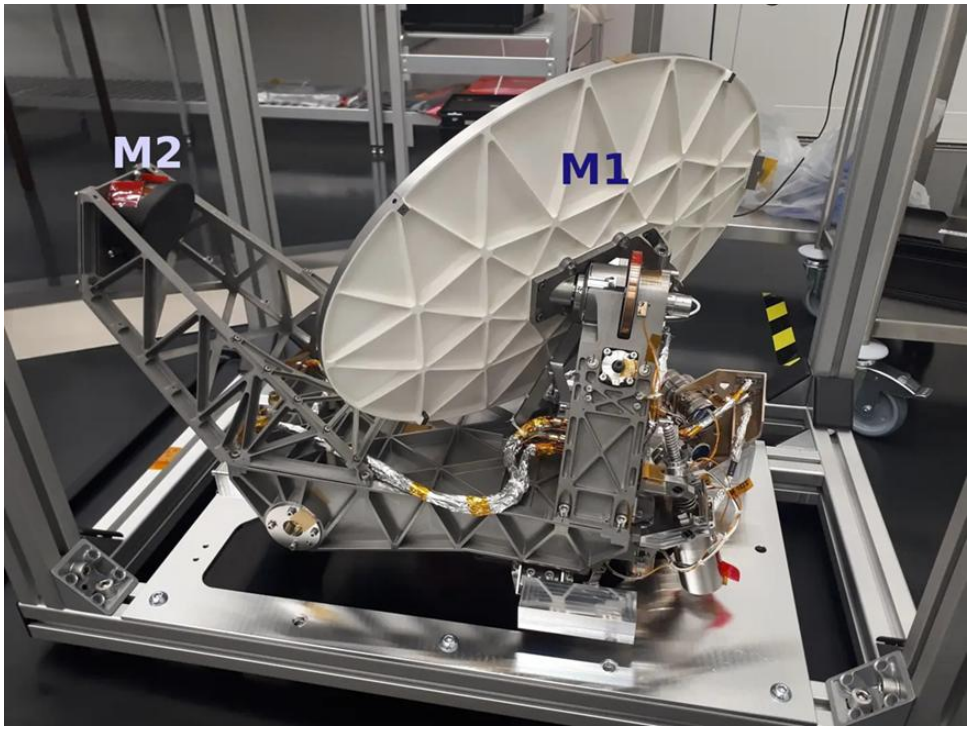

Figure 3: Telescope and receiver unit with M1 and M2 (see text).

The far infrared (submillimetre) signals are first received by a 29 cm diameter mirror (primary, M1, edge taper = 18.7 dB) and then focused by the secondary mirror (M2) into the receiver unit box (see Figures 1, 2 & 3). The M1 of this off-axis Cassegrain telescope can be rotated by ± 72.5 degrees along the ground track of the spacecraft (in the Jupiter orbit) and across the ground track by ± 4.3 degrees with step resolutions of 29.92“ (AT) and 8.67“ (CT), respectively. Therefore, these setups are called along-track (AT) and cross-track (CT) mechanisms. The cross-track scanning range was chosen, because the apparent diameter of Jupiter appears is < 8° for the distances of the spacecraft during the Jupiter tour.

The intermediate frequency signals are connected to the IF&USO distribution unit and feed the wideband Autocorrelation Spectrometer (ACS) and the high-resolution Chirp Transform Spectrometer, (CTS) (Hartogh & Hartmann 1990, Hartogh

1997/1998, Ostrovskyy et al. 2017/18). The bandwidths and channel numbers are 4.4 GHz/1024 and 1 GHz/10000 for the ACS and CTS, respectively.

Figure 4 shows the position of SWI on the spacecraft.

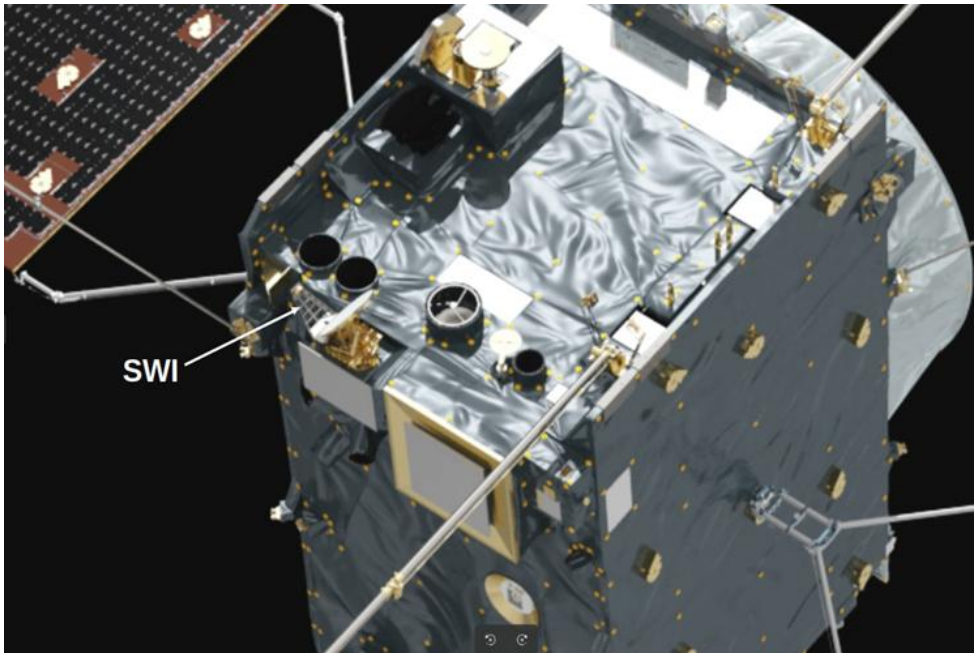

Figure 4: Position of SWI on the Juice spacecraft. Credit: ESA/ATG medialab

3 SWI LEGA in-flight calibration

We leveraged LEGA to acquire observations that supported multiple instrument calibrations: total power, frequency, telescope beam, and pointing. Below we go through the key observations and how they relate to the particular calibration category of SWI. The details are not exhaustive as references to the relevant papers are given (this issue), where appropriate.

3.1 Total power calibration

The goal of total power calibration is to establish the absolute flux (in W/m^2) response of the instrument to far-infrared (FIR)/ submm signals received by the telescope and relate it to brightness temperatures (Rayleigh-Jeans or Planck) of the target. With exactly calibrated fluxes/brightness temperatures we can derive absolute temperatures (atmosphere/surface) and the volume mixing ratio of the detected gases along the line-of-sight of the telescope beam. For calibrating the received FIR-flux, blackbodies with two different temperatures ("cold load" and "hot load") are used. As mentioned above, SWI is using a hot calibration target in the receiver unit (see Figure 2). It is a conical blackbody target that is operated at the environmental temperature of the receiver (typically below 250 K). The temperature of the target is monitored with four platinum resistance thermometers. The target is designed to appear as black as possible, or its emissivity is maximised, by optimising the geometry and by employing a tailored microwave absorbing material (Jacob et al., 2018). This means that reflections causing a temperature bias and standing waves during calibration measurements are suppressed. A signal reflected from the target is attenuated by more than 55 dB. For the cold calibration we are using the cosmic background radiation (2.7 K), by pointing the telescope towards cold space. Beside the blackness of the calibration targets, other parameters play an important role in order to achieve a precise flux calibration. Temperature variations (e.g. caused by the thermal transient response of SWI after switch-on or other instruments being switched on and off or by changes in illumination) will modulate the gain of the instrument. Depending on the amplitude of these gain drifts the flux calibration may be repeated with shorter or longer time intervals. Qualitatively expressed, the amplitude drift of the signal or spectrum shall be smaller than the Gaussian noise on it. This means that highly frequency resolved spectra require less frequent calibrations than e.g. measurements of the continuum. However, for deriving an exact calibration of the total flux, even for highly resolved spectra calibrations have to be repeated typically every few minutes. Unfortunately, we found a lifetime issue of the calibration flip-mirror mechanism after delivery of the instrument to the spacecraft contractor. As a consequence, the number of possible calibration cycles of SWI is reduced to about 5 % of the planned number of calibration cycles. Jarchow et al. (this issue) describes this problem in more detail and reports about work-around approaches of the total power calibration based on LEGA data.

3.2 Frequency calibration

As mentioned in the instrument description, an USO is used as a reference frequency source. After a few hours of operation, it achieves a stability of better than 1E-8 (corresponding to < 10 kHz, a tenth of a spectrometer channel of the CTS). Since one of the science goals of SWI is to measure atmospheric wind speeds using the Doppler shifts of molecular spectral lines, the exact knowledge of the frequency is required. The FDM synthesizers are locked to the USO. The USO absolute frequency is compared with a PPS (Pulse Per Second) signal provided by the spacecraft once per hour. The accuracy of the PPS signal is directly related to the accuracy of the spacecraft time reference (USO). The latter can be calibrated against highly precise frequency standards on ground during the downlink phases of the satellite. The full SWI frequency calibration from the

ground-reference via the spacecraft-USO to the SWI USO is under development. Nevertheless, we learned an important lesson during the LEGA calibration campaign, which is described below.

Figure 5 shows the USO frequency related to the FDM temperature recorded during the Near-Earth Commissioning Phase (NECP**)**. Note that the USO is physically mounted on the FDM. We see a positive correlation between the FDM temperature and the USO frequency of about 2 ppb/°C. The frequency offset against the spacecraft USO is about 700 ppb. Note that here the operational temperature of the FDM is around 0° C, as it was for all payload checkout windows (PCWs) thus far. We did not expect this correlation, because the USO's temperature stabilization should compensate for the temperature variations. For this example, it is obviously not the case. The thermal isolation between FDM and USO or the capability of the USO to compensate temperature variations seems to be not sufficient for this scenario during the NECP (and later during the PCWs). Interestingly we see a somewhat different behavior of the correlation between FDM temperature and USO frequency during LEGA (Figure 6). One difference is the higher operational temperature. While during NECP the FDM temperature varies between -8° C and 6° C, it varies during LEGA between about 0° C and 22° C. The other striking difference is that above about 15° C the USO internal temperature regulation seems to be able to compensate the temperature change of the FDM and the positive correlation between FDM temperature and USO frequency disappears.

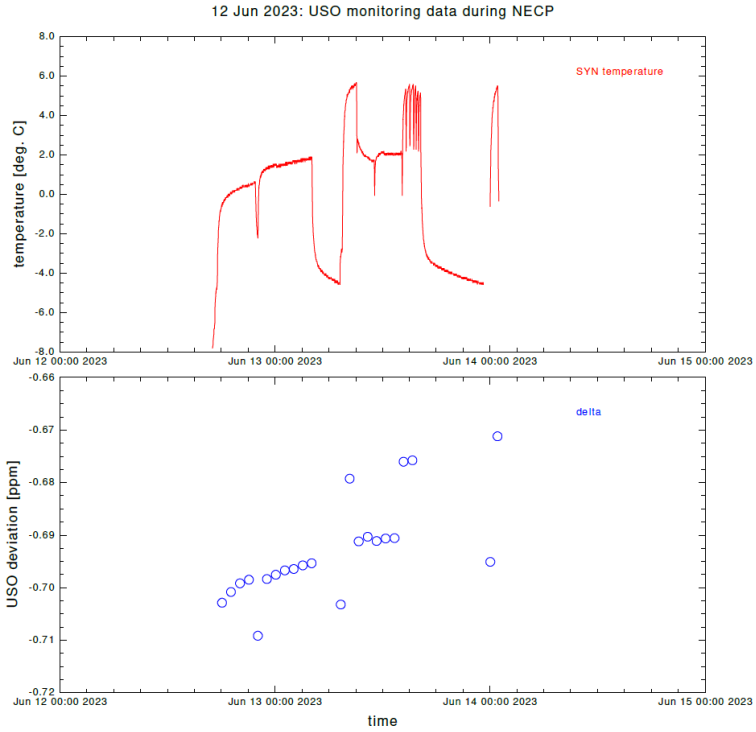

Figure 5: Temperature variation of the FDM (upper panel) and related frequency variation of the USO (lower panel) during NECP.

As mentioned before, the SWI-USO is referenced against the spacecraft USO once an hour. Our understanding is that the spacecraft-USO is switched-on all the time. Therefore, it is likely that its stability is superior to the SWI-USO, which is switched off after each PCW and flyby. Further analysis on the spacecraft USO stability against the ground station reference has to be performed in order to confirm or disprove this assumption.

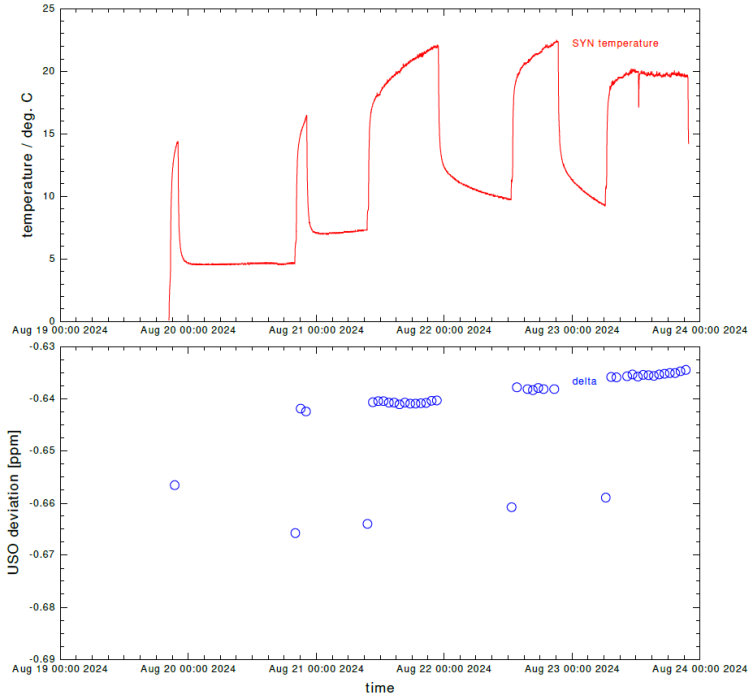

Figure 6: Temperature variation of the FDM (upper panel) and related frequency variation of the USO (lower panel) during LEGA

The above-mentioned end-to-end frequency calibration development will include:

- Quantification of the change in correlation between the FDM temperature and the SWI-USO for a larger operational temperature range
- Estimate of the drift of the SWI-USO within the 1 h calibration intervals
- Estimate the drift of the spacecraft USO within the spacecraft to ground calibration intervals.

A detailed description of the end-to-end frequency calibration scheme and the analyses of the drift behavior of the spacecraft USO and the SWI-USO and its impact on the science requirements will be described later in a dedicated paper.

3.3 Telescope beam calibration

The knowledge of the telescope beam function is of importance for a number of observations. The diameter of the main beam (main lobe) is a measure for the spatial resolution of the intended observations. In case the observed object is not resolved, the main beam size determines e.g. the strength, or line intensities of the observed molecular spectra in the atmospheres of Jupiter and the Galilean satellites and has a direct impact on the required observation times and thus for the operational planning. The knowledge of the second and higher order sidelobes is of importance for a number of observational scenarios. For example, if the main beam is pointed to cold space, SWI may still detect a much brighter molecular spectrum from Jupiter's atmosphere through its second or higher sidelobes, which leads to ambiguous results.

In order to characterize the telescope beam, so-called nearfield measurements were performed on ground in the new Low-temperature Near-field Terahertz chamber (LORENTZ) at ESTEC in Noordwijk. These measurements had a dynamic range of > 50 dB allowing to determine the telescope pattern to beyond the 10^{th} sidelobe. We determined a half-power beamwidth of the main lobe of 7.85' at 600 GHz and 4.3' at 1200 GHz.

During LEGA and former campaigns (NECP, PCWs) we tried to verify in the farfield the results from the ground-based nearfield measurements. The idea behind the measurements in space is to x-y scan over a celestial object (e.g. Earth and Moon) from a large distance so that the object is at least 5 x smaller than the diameter of the main beam and then deconvolve the result of the x-y scan. The disadvantage of these farfield measurements compared to nearfield measurements is that the sources' (Earth/moon) fluxes are small compared to the transmitters used for the nearfield measurements. Since the THz temperatures are to first order proportional to the physical temperature of Earth and the Moon, dynamic ranges of 20 to 23 dB can be achieved allowing to characterize the main lobe and perhaps the first side lobe. Using the Sun as THz source would increase the dynamic range to ~36 dB so that even the 5^{th} sidelobe could be characterized, however the diameter of the Sun is too large for this approach, even from the Jupiter system, instead it would require distances > 40 AU from the Sun. The results from LEGA in determining the telescope beam and whether it is compatible with the nearfield results are described in Moreno et al., this issue.

3.4 Pointing calibration

The exact pointing knowledge is essential for a number of SWI science operations, e.g. the determination of line-of-sight winds in the Jupiter system. The original SWI requirement of the pointing knowledge was 5". In order to achieve 5" pointing knowledge, in the original telescope design an angular encoder was included. Due to schedule problems the project recommended to descope the encoder. Without the angular encoder the pointing knowledge is limited by the step size and accuracy of the along track mechanism, i.e. about 6-10 times larger. Therefore, a pointing calibration is required, e.g. in scanning over the limb of Jupiter following a dedicated algorithm. LEGA offered the opportunity to test the approach, although

the exact algorithm is still not running reliably in the application software. The pointing calibration is a rather complex procedure, and we did not have enough time to analyse the pointing data of LEGA in detail and the final results of LEGA concerning pointing calibration will be published later. Nevertheless, first results will be presented in Moreno et al, this issue.

4 LEGA operations

SWI observation planning activities encompass both the cruise phase and the Jupiter science phase, each presenting distinct operational challenges. The preparation of LEGA observations provided our first comprehensive insight into the complexity of this process, highlighting key aspects, such as scheduling, geometry and script configuration, etc. This led us to identify processes that can be made more robust by automation. The operations include 9 calibration modes and 22 science observation modes. The observation planning is a complex process. Its complexity required the development of a SWI specific observation planning tool that allows to perform a number of dedicated observation strategies for the different phases of the Juice trajectory. Details about SWI operations are summarized in the paper of Cavalié et al., this issue.

5 Conclusions

We provide an introduction and overview about the initial SWI LEGA characterization, operation, and in-flight calibration of SWI during the LEGA campaign. The fundamental functions and specifications of SWI are described followed by a short introduction on the calibrations we intended to perform based on data acquired during LEGA. A preliminary analysis on the frequency calibration is provided. For detailed analyses on total power and beam calibration and the observation and operations planning we refer to three other SWI papers prepared for this special issue of ANGEO on LEGA.

Data availability

The SWI data acquired during the JUICE Moon–Earth gravity assist in August 2024 are currently under the mission's cruise-phase proprietary period. These data will be made available through the ESA Planetary Science Archive following the first Cruise Archive Delivery, which is currently scheduled for six months after the third Earth Gravity Assist in 2029

hat formatiert: Schriftart: Kursiv

Author contributions

Author contributions. P. Hartogh prepared the original manuscript. L. Rezac, C. Jarchow, A. Schulz-Ravanbakhsh, T. Cavalié, R. Moreno, and P. Hartogh defined the LEGA operational strategy for SWI. All co-authors contributed to the successful implementation of SWI and provided critical feedback on the manuscript.

Competing interests

The authors declare no competing interests.

Acknowledgements

SWI has been designed and developed by an international consortium of institutes led by the Max Planck Institute for Solar System Research (MPS, Germany) and including the Observatoire de Paris, Laboratory for Studies of Radiation and Matter in Astrophysics (LERMA, France), the Space Research Centre of the Polish Academy of Sciences (CBK PAN, Poland), Chalmers University of Technology (Sweden), the Institute of Applied Physics of the University of Bern (IAP, Switzerland), the National Institute of Information and Communications Technology (NICT, Japan) and the French Space Agency CNES with additional support from the Laboratoire d'Instrumentation et de Recherche en 620 Astrophysique of the Observatoire de Paris (LIRA, France), the Laboratoire d'Astrophysique de Bordeaux (LAB, France), the RPG Radiometer Physics GmbH (Germany), and Omnisys Instrument AV (Sweden). This development has been supported by national funding agencies and other organizations, including the Deutsches Zentrum fur Luft- und Raumfahrt (DLR) and by central resources of the Max Planck Society. T. Cavalié and F. Herpin acknowledge funding from the Centre National d'Etudes Spatiales (CNES). E.S. Wirström acknowledges generous support from the Swedish National Space Agency. Juice is a mission under ESA leadership with contributions from its Member States, NASA, JAXA, and the Israel Space Agency. It is the first Large-class mission (L1) in ESA's Cosmic Vision Program.

References

Beaudin, G., Gulkis, S., Frerking, M., Hartogh, P., Allen, M., Bockelee-Morvan, D. Crovisier, J., Despois, D., Encrenaz, P., Encrenaz, T., Germain, B., Hofstadter, M., Ip, W., Janssen, M., Lellouch, E., Mann, I., Muhleman, D., Rauer, H., Schloerb, F.P., and Spilker, T: A microwave radiometer/spectrometer for the ROSETTA orbiter, in: Proceedings of the 2nd ESA Workshop on Millimetre Wave Technology and Applications: Antennas, Circuits and Systems (edited by J. Mallat, A. Räisänen, and J. Tuovinen), pp. 43–48, ESA WPP-149, ESA Publ. Div., ESPOO, Finland, 1998.

Boutonnet, A., Langevin, Y., and Erd, C.: Designing the JUICE Trajectory, 220, 67, https://doi.org/10.1007/s11214-024-01093-y, 2024.

Cavalié, T., Benmahi, B., Hue, V., Moreno, R., Lellouch, E., Fouchet, T., Hartogh, P., Rezac, L., Greathouse, T. K., Gladstone, G. R., Sinclair, J. A., Dobrijevic, M., Billebaud, F., and Jarchow, C.: First direct measurement of auroral and equatorial jets in the stratosphere of Jupiter: 647, L8, https://doi.org/10.1051/0004-6361/202140330, 2021

Cavalié, T., Rezac, L., Moreno, R., Lellouch, E., Fouchet, T., Benmahi, B., Greathouse, T. K., Sinclair, J. A., Hue, V., Hartogh, P., Dobrijevic, M., Carrasco, N., and Perrin, Z.: Evidence for auroral influence on Jupiter's nitrogen and oxygen chemistry revealed by ALMA, Nature Astronomy, 7, 1048–1055, https://doi.org/10.1038/s41550-023-02016-7, 2023.

Cavalié, T.,Moreno, R., Rezac, L., Herpin, F.,Jarchow, C. Hartogh, P., Carrasco Gallardo, A., Goodyear, S., Pierre Mancini, P., Schulz-Ravanbakhsh, A. , Dabrowski, B., Kasai, Y., Lellouch, E., Murk, A., Murtagh, D., Olberg, M., Rengel, M., Sagawa, H., Szutowicz, S. and Wirström, E.: Juice-SWI during the Lunar-Earth-Gravity-Assist (LEGA). II. Instrument operations, Ann. Geophys., This issue, 2026

Fletcher, L. N., Cavalié, T., Grassi, D., Hueso, R., Lara, L. M., Kaspi, Y., Galanti, E., Greathouse, T. K., Molyneux, P. M., Galand, M., Vallat, C., Witasse, O., Lorente, R., Hartogh, P., Poulet, F., Langevin, Y., Palumbo, P., Gladstone, G. R., Retherford, K. D., Dougherty, M. K., Wahlund, J.-E., Barabash, S., Iess, L., Bruzzone, L., Hussmann, H., Gurvits, L. I., Santolik, O., Kolmasova, I., Fischer, G., Müller-Wodarg, I., Piccioni, G., Fouchet, T., Gérard, J.-C., Sánchez-Lavega, A., Irwin, P. G. J., Grodent, D., Altieri, F., Mura, A., Drossart, P., Kammer, J., Giles, R., Cazaux, S., Jones, G., Smirnova, M., Lellouch, E., Medvedev, A. S., Moreno, R., Rezac, L., Coustenis, A., and Costa, M.:Jupiter Science Enabled by ESA's Jupiter Icy Moons Explorer, Space Sci. Rev., 219, 53, https://doi.org/10.1007/s11214-023-00996-6,145 , 2023.

de Graauw, T., Whyborn, N. D., van de Stadt, H., Beaudin, G., Beintema, D. A., Belitsky, V., Cais, P., Caux, E., Gheudin, M., Cros, A., de Groene, P., Emrich, A., Erickson, N. R., Gaier, T. C., Gallego-Puyol, J. D., Gao, J., Hartogh, P., Honingh, N., Horn, J., Jacobs, K., Kruisinga, R., Lura, F., Lecacheux, A., Natale, V., Orfei, R., Pearson, J. C., Phillips, T. G., Roelfsema, P. R., Rosolen, C., Salez, M., Schieder, R. T., Schuster, K.-F., Schwaab, G. W., Starsky, J. P., Stutzki, J., Torchinsky, S., van Leeuwen, B., Visser, H., Wildeman, K. J., Withington, S., and Zmuidzinas, J.: Heterodyne instrument for FIRST (HIFI): preliminary design, in: Advanced Technology MMW, Radio,and Terahertz Telescopes, edited by Phillips, T. G., vol. 3357 of Society of Photo-Optical Instrumentation Engineers (SPIE) Conference Series, pp. 336–347, https://doi.org/10.1117/12.317368, 1998.

de Graauw, T., Helmich, F. P., Phillips, T. G., Stutzki, J., Caux, E., Whyborn, N. D., Dieleman, P., Roelfsema, P. R., Aarts, H., Assendorp, R., Bachiller, R., Baechtold, W., Barcia, A., Beintema, D. A., Belitsky, V., Benz, A. O., Bieber, R., Boogert, A., Borys, C., Bumble, B., Caïs, P., Caris, M., Cerulli-Irelli, P., Chattopadhyay, G., Cherednichenko, S., Ciechanowicz, M., Coeur-Joly, O., Comito, C., Cros, A., de Jonge, A., de Lange, G., Delforges, B., Delorme, Y., den Boggende, T., Desbat, J.-M., Diez-González, C., di Giorgio, A. M., Dubbeldam, L., Edwards, K., Eggens, M., Erickson, N., Evers, J., Fich, M., Finn, T., Franke, B., Gaier, T., Gal, C., Gao, J. R., Gallego, J.-D., Gauffre, S., Gill, J. J., Glenz, S., Golstein, H., Goulooze, H., Gunsing, T., Güsten, R., Hartogh, P., Hatch, W. A., Higgins, R., Honingh, E. C., Huisman, R., Jackson, B. D., Jacobs, H., Jacobs, K., Jarchow, C., Javadi, H., Jellema, W., Justen, M., Karpov, A., Kasemann, C., Kawamura, J., Keizer, G., Kester, D., Klapwijk, T. M., Klein, T., Kollberg, E., Kooi, J., Kooiman, P.-P., Kopf, B., Krause, M., Krieg, J.-M., Kramer, C., Kruizenga, B., Kuhn, T., Laauwen, W., Lai, R., Larsson, B., Leduc, H. G., Leinz, C., Lin, R. H., Liseau, R., Liu, G. S., Loose, A., López-Fernandez, I., Lord, S., Luinge, W., Marston, A., Martín-Pintado, J., Maestrini, A., Maiwald, F. W., McCoey, C., Mehdi, I., Megej, A., Melchior, M., Meinsma, L., Merkel, H., Michalska, M., Monstein, C., Moratschke, D., Morris, P., Muller, H., Murphy, J. A., Naber, A., Natale, E., Nowosielski, W., Nuzzolo, F., Olberg, M., Olbrich, M., Orfei, R., Orleanski, P., Ossenkopf, V., Peacock, T., Pearson, J. C., Peron, I., Phillip-May, S., Piazzo, L., Planesas, P., Rataj, M., Ravera, L., Risacher,

C., Salez, M., Samoska, L. A., Saraceno, P., Schieder, R., Schlecht, E., Schlöder, F., Schmülling, F., Schultz, M., Schuster, K., Siebertz, O., Smit, H., Szczerba, R., Shipman, R., Steinmetz, E., Stern, J. A., Stokroos, M., Teipen, R., Teyssier, D., Tils, T., Trappe, N., van Baaren, C., van Leeuwen, B.-J., van de Stadt, H., Visser, H., Wildeman, K. J., Wafelbakker, C. K., Ward, J. S., Wesselius, P., Wild, W., Wulff, S., Wunsch, H.-J., Tielens, X., Zaal, P., Zirath, H., Zmuidzinas, J., and Zwart, F.: The Herschel-Heterodyne Instrument for the Far-Infrared (HIFI), 518, L6, https://doi.org/10.1051/0004-6361/201014698, 2010.

Grasset, O., Dougherty, M. K., Coustenis, A., Bunce, E. J., Erd, C., Titov, D., Blanc, M., Coates, A., Drossart, P., Fletcher, L. N., Hussmann, H., Jaumann, R., Krupp, N., Lebreton, J.-P., Prieto-Ballesteros, O., Tortora, P., Tosi, F., and Van Hoolst, T.: JUpiter ICy moons Explorer (Juice): An ESA mission to orbit Ganymede and to characterise the Jupiter system, , 78, 1–21, https://doi.org/10.1016/j.pss.2012.12.002, 2013.

Guesten, R., Hartogh, P., Huebers, H.-W., Graf, U. U., Jacobs, K., Roeser, H.-P., Schaefer, F., Schieder, R. T., Stark, R., Stutzki, J., Van der Wal, P., and Wunsch, A.: GREAT: the first-generation German heterodyne receiver for SOFIA, in: Airborne Telescope Systems, edited by Melugin, R. K. and Röser, H.-P., vol. 4014 of Society of Photo-Optical Instrumentation Engineers (SPIE) Conference Series, pp. 23–30, https://doi.org/10.1117/12.389122, 2000.

Gulkis, S., Frerking, M., Crovisier, J., Beaudin, G., Hartogh, P., Encrenaz, P., Koch, T., Kahn, C., Salinas, Y., Nowicki, R., Irigoyen, R., Janssen, M., Stek, P., Hofstadter, M., Allen, M., Backus, C., Kamp, L., Jarchow, C., Steinmetz, E., Deschamps, A., Krieg, J., Gheudin, M., Bockelée-Morvan, D., Biver, N., Encrenaz, T., Despois, D., Ip, W., Lellouch, E., Mann, I., Muhleman, D., Rauer, H., Schloerb, P., and Spilker, T.: MIRO: Microwave Instrument for Rosetta Orbiter, Space. Sci. Rev., 128, 561–597, https://doi.org/10.1007/s11214-006-9032-y, 2007.

Hartogh, P. and Hartmann, G. K.: A high-resolution chirp transform spectrometer for microwave measurements, Measurement Science and Technology, 1, 592–595, https://doi.org/10.1088/0957-0233/1/7/008, 1990.

Hartogh, P.: Present and future chirp transform spectrometers for microwave remote sensing, in: Sensors, Systems, and Next-Generation Satellites, edited by Fujisada, H., vol. 3221 of Society of Photo-Optical Instrumentation Engineers (SPIE) Conference Series, pp. 328–339, https://doi.org/10.1117/12.298099, 1997

Hartogh, P.: A new microwave heterodyne spectrometer backend: The ASIC-CTS, in: Proceedings of the 2nd ESA Workshop on Millimetre Wave Technology and Applications: Antennas, Circuits and Systems (edited by J. Mallat, A. Räisänen, and J. Tuovinen), pp. 333–338, ESA WPP-149, MilliLab, ESPOO, Finland, 1998.

Hartogh, P., Lellouch, E., Rezac, L., and others: SubmillimetreWave Instrument (SWI) on board ESA's Jupiter Icy Moons Explorer (Juice), Space Sci. Rev., in prep, 2026a.

Heyminck, S., Graf, U. U., Güsten, R., Stutzki, J., Hübers, H. W., and Hartogh, P.: GREAT: the SOFIA high-frequency heterodyne instrument, 542, L1, https://doi.org/10.1051/0004-6361/201218811, 2012.

Ilyushin, Y. A. and Hartogh, P.: Submillimeter Wave Instrument radiometry of the Jovian icy moons. Numerical simulation of the microwave thermal radiative transfer and Bayesian retrieval of the physical properties, 644, A24, https://doi.org/10.1051/0004-6361/201937220, 2020.

Jacob, K., Schröder, A., and Murk, A.: Design, Manufacturing, and Characterization of Conical Blackbody Targets With Optimized Profile, IEEE Transactions on Terahertz Science and Technology, 8, 76–84, https://doi.org/10.1109/TTHZ.2017.2762309, 2018.

Jarchow, C., Rezac, L., Hartogh, P., Schulz-Ravanbakhsh, A., Cavalié, T., and Moreno, R.: Observations of the Earth as Calibration Target for Juice/SWI during the Lunar-Earth-Gravity-Assist, Ann. Geophys., this issue, 2026.

Kotiranta, M., Jacob, K., Kim, H., Hartogh, P., and Murk, A.: Optical Design and Analysis of the Submillimeter-Wave Instrument on Juice, IEEE Transactions on Terahertz Science and Technology, 8, 588–595, https://doi.org/10.1109/TTHZ.2018.2866116, 2018.

Moreno R., Ladislav R., Formánek T., Cavalié T., Jarchow, C., Lellouch, E., Hartogh, P., Murk, A., Kotiranta, M., Carrasco Gallardo, A., Goodyear, S., Schulz-Ravanbakhsh, A., Dabrowski, B., Herpin, F., Kasai, Y., Murtagh, D., Olberg, M., Rengel, M., Sagawa, H-, Szutowicz, S., and Wirström, E.: Pointing and bean characterization of Juice/SWI during the Lunara-Earth Gravity Assist, Ann. Geophys., this issue, 2026.

Ostrovsky, P.; Tittelbach-Helmrich, K.; Herzel, F.; Schrape, O.; Fischer, G.; Kissinger, D.; Börner, P.; Loose, A.; Hellmann, D.; Hartogh, P.: A single chip 16 GS/s arbitrary waveform generator in 0.13 µm BiCMOS technology. In: 2017 IEEE Nordic Circuits and Systems Conference (NORCAS): NORCHIP and International Symposium of System-on-Chip (SoC). 2017 IEEE Nordic Circuits and Systems Conference (NORCAS): NORCHIP and International Symposium of System-on-Chip (SoC) , Linkoping, Sweden , October 23, 2017. (2017)

Ostrovskyy, P.; Schrape, O.; Tittelbach-Helmrich, K.; Herzel, F.; Fischer, G.; Hellmann, D.; Börner, P.; Loose, A.; Hartogh, P.; Kissinger, D.: A Radiation Hardened 16 GS/s Arbitrary Waveform Generator IC for a Submillimeter Wave Chirp-Transform Spectrometer. In: 2018 IEEE Nordic Circuits and Systems Conference (NORCAS): NORCHIP and International Symposium of System-on-Chip (SoC) (Eds. Nurmi, J.; Ellervee, P.; Mihhailov, J.; Jenihhin, M.; Tammemäe, K.). 2018 IEEE Nordic Circuits and Systems Conference (NORCAS): NORCHIP and International Symposium of System-on-Chip (SoC) , Tallinn, Estonia, October 30, 2018 - October 31, 2018. (2018).

Tosi, F., Roatsch, T., Galli, A., Hauber, E., Lucchetti, A., Molyneux, P., Stephan, K., Achilleos, N., Bovolo, F., Carter, J., Cavalié, T., Cimò, G., D'Aversa, E., Gwinner, K., Hartogh, P., Huybrighs, H., Langevin, Y., Lellouch, E., Migliorini, A., Palumbo, P., Piccioni, G., Plaut, J. J., Postberg, F., Poulet, F., Retherford, K., Rezac, L., Roth, L., Solomonidou, A., Tobie, G., Tortora, P., Tubiana, C., Wagner, R., Wirström, E., Wurz, P., Zambon, F., Zannoni, M., Barabash, S., Bruzzone, L., Dougherty, M., Gladstone, R., Gurvits, L. I., Hussmann, H., Iess, L., Wahlund, J.-E., Witasse, O., Vallat, C., and Lorente, R.: Characterization of the Surfaces and Near-Surface Atmospheres of Ganymede, Europa and Callisto by JUICE, 220, 59, https://doi.org/10.1007/s11214-024-01089-8, 2024.

Treuttel, J., Gatilova, L., Caroopen, S., Feret, A., Gay, G., Vacelet, T., Valentin, J., Jin, Y., Cavanna, A., Jacob, K. F., Mignoni, S., Lavignolle, V., Krieg, J.-M., Goldstein, C., Courtade, F., Larigauderie, C., Ravanbakhsh, A., Garcia, J.-P., Maestrini, A. E., and Hartogh, P.: 1200 GHz High Spectral Resolution Receiver Front-End of Submillimeter Wave Instrument for JUpiter

ICy Moon Explorer: Part I - RF Performance Optimization for Cryogenic Operation, IEEE Transactions on Terahertz Science and Technology, 13, 324–336, https://doi.org/10.1109/TTHZ.2023.3263623, 2023.

Wirström, E. S., Bjerkeli, P., Rezac, L., Brinch, C., and Hartogh, P.: Effect of the 3D distribution on water observations made with the SWI. I. Ganymede: 637, A90, https://doi.org/10.1051/0004-6361/202037609, 2020.